Supplementary Clinical Descriptions

Clinical descriptions of individuals with *CTNNB1* mutations

Patient 1

This boy was born after an uncomplicated pregnancy and delivery with a normal birth weight. In the neonatal period he was restless. His psychomotor development was delayed from the beginning and he had a low muscle tone. After the age of 18 months he learnt to sit independently. At the age of 30 months he was not able to walk or speak, and had feeding difficulties (chewing, swallowing). He communicated with pictograms. His vision was impaired due to hypermetropia. At the age of four years and six months he was able to walk short distances, but preferred to move forward on his knees. He could speak some sentences, but he articulated poorly and was hard to understand. In general his health condition was good and he had a happy personality. A cerebral MRI at the age of 1 year revealed corpus callosum hypoplasia. His TIQ measured at age 4 years, was 72. Upon physical examination at the ages of 18 months, 30 months and 4 years, 6 months he had a steady microcephaly. At the age of 4 years and 6 months, his heigth was 107 cm (50^{th} centile), weight 14.9 kg (3^{rd} centile) and skull circumference (SC) 46.5 cm (0.1^{th} centile). His big toes were rather broad. A cerebral MRI at the age of 1 year revealed corpus callosum hypoplasia. Facial dysmorphisms at the age of 4 years and 6 months are shown in Figure 1E. SNP array analysis, DNA diagnostic tests for Prader Willi syndrome and mutation analysis of *CREBBP* and *EP300* were normal.

Patient 2

This female was born after an uncomplicated pregnancy and birth. She was the second child in a family of three children. The parents were not related. At the age of 6 months her development showed a regression and the parents noticed hypotonia. Since then she showed a very slow progression in cognitive development. After the age of two years she learnt to sit without support

and she was three years of age when she started to crawl. At the age of 12 years she could walk with little support, but she never learnt to walk independently due to a slowly progressive spasticity. She started to speak her first words between the age of 9 and 10 years. Behavior problems included aggression, automutilation and fecal smearing. Her general health condition was rather good. Upon ascertainment at the age of 29 years she had a moderate to severe intellectual disability and was able to speak a few single words. She had a height of 153 cm (0.6th centile), weight of 58.6 kg (50th centile) and microcephaly (head circumference of 51.2 cm, 0.6th centile). The hands were fleshy with broad fingers. She was hypertonic and could only walk a few steps on her toes and had a severe scoliosis. Facial dysmorphisms are shown in Figure 1E. SNP array analysis, tests for Rett-like syndromes (*MECP2, FOXG1, CDKL5)*, testing of *CREBBP* and *EP300*, and a metabolic screen in blood and urine were normal.

Patient 3

This female was born after an uncomplicated pregnancy and birth. In the neonatal period she was slow to feed and cried a lot. Her motor development was delayed and she only learnt to walk with the support of a walking frame. She did not learn to speak, but was able to use sign language. Over the years her motor skills gradually declined, she became progressively spastic, and at the age of 50 years she was no longer able to walk. In addition she had progressive swallowing difficulties. Her cognitive abilities and contact making gradually deteriorated as well. Opthalmologic evaluation had revealed a slight atrophy of the right optic nerve and moderate hypoplasia of the left optic papilla. Upon physical examination at the age of 51 years she was a severely disabled woman who was fully wheelchair dependent and slow to response. She had a low to normal height (162 cm, <25 th centile) and weight (56 kg, 50th centile) and microcephaly (50.4 cm, <0.6th centile). Hands and feet were normal. Facial dysmorphisms are shown in Figure 1E. SNP array analysis on blood lymphocytes was reported to be normal. SNP array analysis on bucchal cells showed a mosaic gain in 2q34 (209.25-

210.28, Hg17), sized approximately 1 Mb, with unknown, significance, but unlikely to explain the severe ID phenotype. A metabolic screen in blood revealed no abnormalities.

Patient 4

This female was the third child of healthy parents and had two healthy sisters. Pregnancy was complicated by intra-uterine growth retardation during the third trimester. Birth was uncomplicated, but she had a low birth weight (2,510 grams, 2.3th centile) and a primary microcephaly (32 cm at 40 weeks duration of pregnancy). The neonatal period was complicated by temperature dysregulation, hypotonia, feeding difficulties and excessive crying. The parents had noticed a developmental delay since the age of six months. She learned to sit without support after the age of 12 months, learned to walk at the age of 4,5 years and started to babble at the age of 3 years. At the age of 13 months she was operated on strabismus. In addition she was diagnosed with a spastic diplegia of the lower extremities. She walked with the support of a walking frame and used a wheelchair for longer distances. At the age of 7 years an intelligence test gave an IQ score of 65. At the age of 14 years she was able to speak in simple sentences and was able to read simple words. Her overall intellectual functioning corresponded to a level of mild to moderate ID. She showed features of autism spectrum disorder and she was not yet fully toilet trained.

Her general health condition was good, except from a period with recurrent upper airway infections during infancy. During puberty she developed a scoliosis.

Upon physical examination at the age of 14 years, she made a younger impression. She had a dystrophic build. Her height was 161 cm (25th-50th centile), her weight was 34.8 kg (<0.6th centile according to height), and her head circumference was 49 cm (<<0.6th centile). Facial dysmorphisms are shown in Figure1E. SNP array analysis, DNA diagnostic tests for Angelman- and Rett syndrome (methylation analysis, *UBE3A* and *MECP2*), and a metabolic screen in blood and urine revealed no explanation for her phenotype.

Supplementary Material

Supplementary Methods

Allele-specific amplification of mRNA

For the nonsense-mediated decay (NMD) study, Epstein Barr virus (EBV)-transformed B cells from individual subjects were used. 1 to 5 micrograms of total RNA were isolated from cell suspensions of approximately $1x10^6$ cells using the NucleoSpin RNA II RNA isolation kit (Machery-Nagel). RNA was quantified by UV absorbance (A260/280 ratio) and checked by gel electrophoresis. RT-PCR was performed by amplifying the relevant region of RNA from appropriate cell lines treated with (+) cycloheximide (CHX) to inhibit NMD or without (-) CHX. The primers used were: Patient 1 (p.Gln309X), Fw 5'-gcgttctcctcagatggtgt, Rv 5'-gggtccaccactagccagtat; Patient 2 (p.Ser425ThrfsX11), Fw 5'-aacaggaagggatggaaggt, Rv 5'-agtgggatggtgggtgtaag.

Hematoxylin and eosin staining

Brains were prepared for fixation (Thermo Shandon Pathcentre), embedded in paraffin (Thermo Scientific Histo Star) and cut in 5µm thick sections (Finesse). Overview staining with hematoxylin and eosin was performed using a standard program on the Sakura Tissue-Tek DRS machine. Samples were visualised with the Axio-Observer microscope (Zeiss, Jena, Germany) using the respective software and the MosaiX application and a 10x objective (Plan-apochromat 10x NA 0.3).

Supplementary Figures

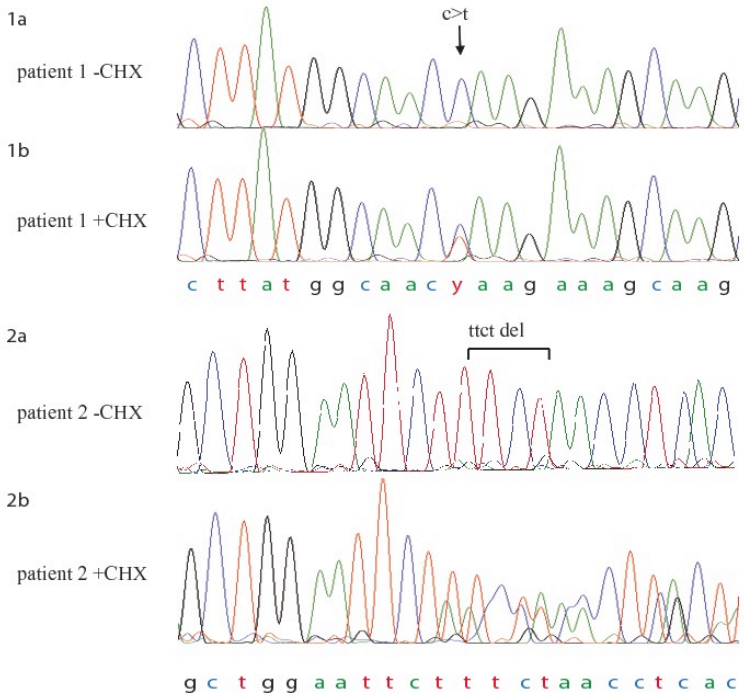

Figure S1. Chromatograms showing degradation of the mutant *CTNNB1* alleles in individuals 1 and 2, suggestive of nonsense-mediated mRNA decay (NMD). Sequence was derived from RT-PCR amplifying the relevant region from RNA derived from lymphoblastoid cell lines treated with (+) or without (-) cycloheximide (CHX) to inhibit NMD. 1a,b: *CTNNB1* (hg19) g.41267341 C>T; c.925 C>T; p.(Gln309*) (patient 1); 2a,b: *CTNNB1* (hg19) g.41275106_41275109del; c.1272_1275TTCTdel; p.(Ser425ThrfsX11) (patient 2).

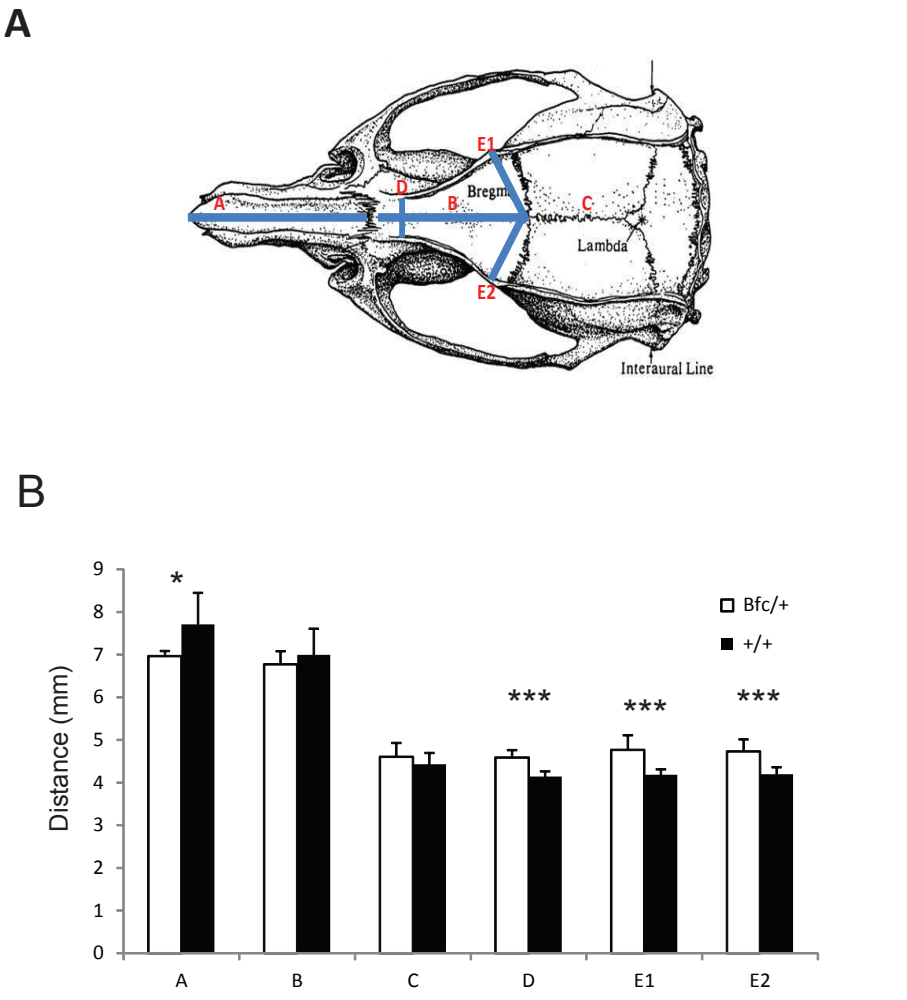

Figure S2. Measurement of skull bone length and width in *+/+* and *Bfc/+* adults. Bone measurements were recorded as depicted in **A)**. **B)** Comparison of multiple measurements in *+/+* (mean ± sem, n=9) and *Bfc/+* (mean ± sem, n=8) mice. (Student's t-test: *p<0.05, ***p<0.001).

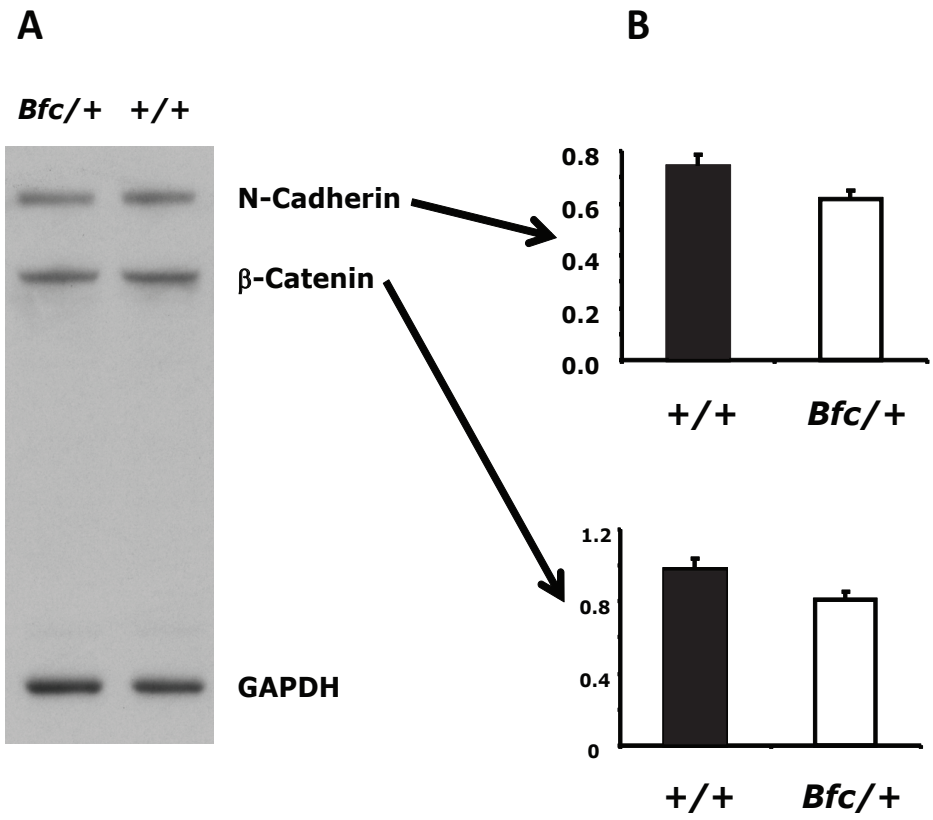

Figure S3. N-cadherin and β-catenin levels in wild-type and heterozygous batface whole hippocampal lysates. A). Representative Western blot showing hippocampal immunoreactivity for N-cadherin, β-catenin and the loading control GAPDH from the same sample. **B).** Multiple runs were quantified and relative protein levels determined by densitometry (mean $\pm$ sem, n=5). The levels of both N-cadherin and β-catenin were not significantly different among genotypes ($p = 0.195$ and $p=0.098$ for N-cadherin and β-catenin respectively).

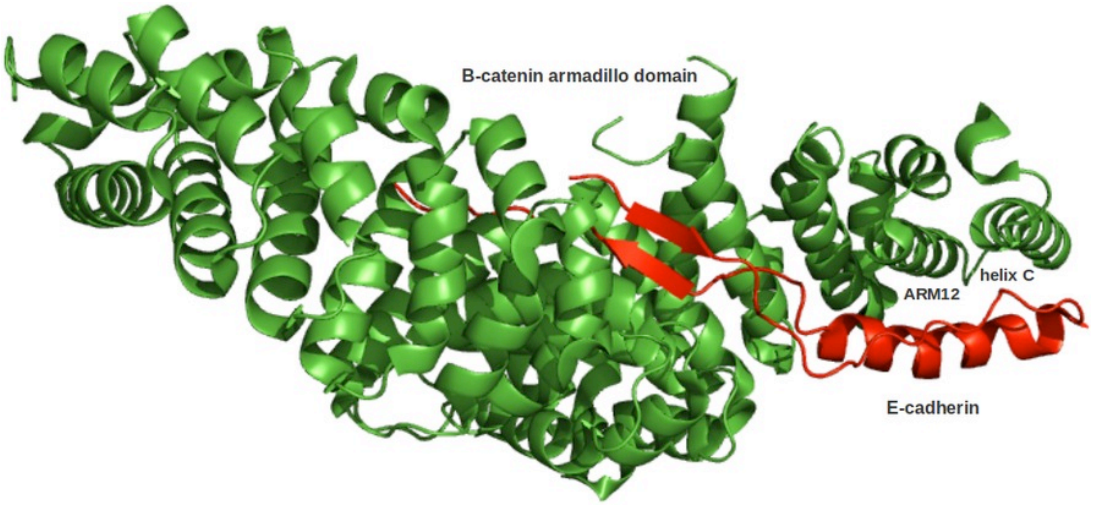

Figure S4. The crystal structure of the murine β-catenin and E- cadherin complex - PDB 2z6h
The armadillo domain of β-catenin (green cartoon view) encompasses arm repeats ARM1 to ARM 12. Five interaction regions comprise the E-cadherin cytoplasmic domain (red cartoon view) with each region contacting specific arm repeats (1).

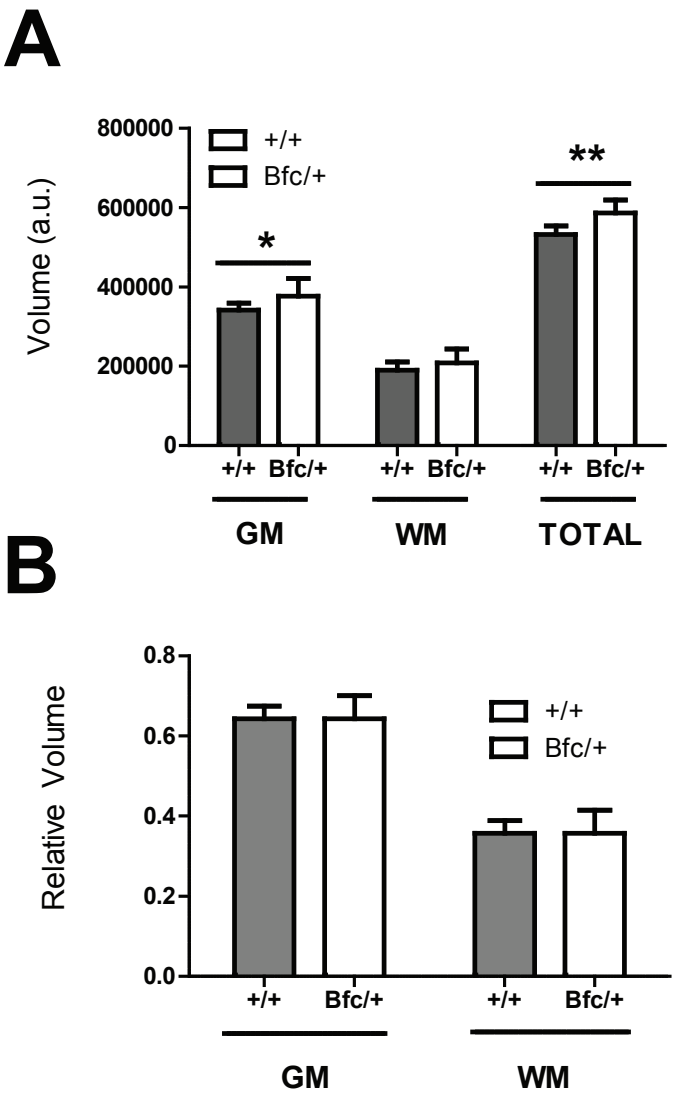

Figure S5. Differences in brain volume measurements detected using MRI. (**A**) Mean gray-matter (GM), white matter (WM) and total brain volume (TOTAL) in *Bfc/+* mice and control littermates as measured with MRI (mean ± sem). *p<0.05, ** p<0.01 vs. control; one-way ANOVA. (**B**). Normalised GM and WM volumes in *Bfc/+* mice and control littermates. Normalised values were computed by dividing individual GM and WM volumes by total brain size.

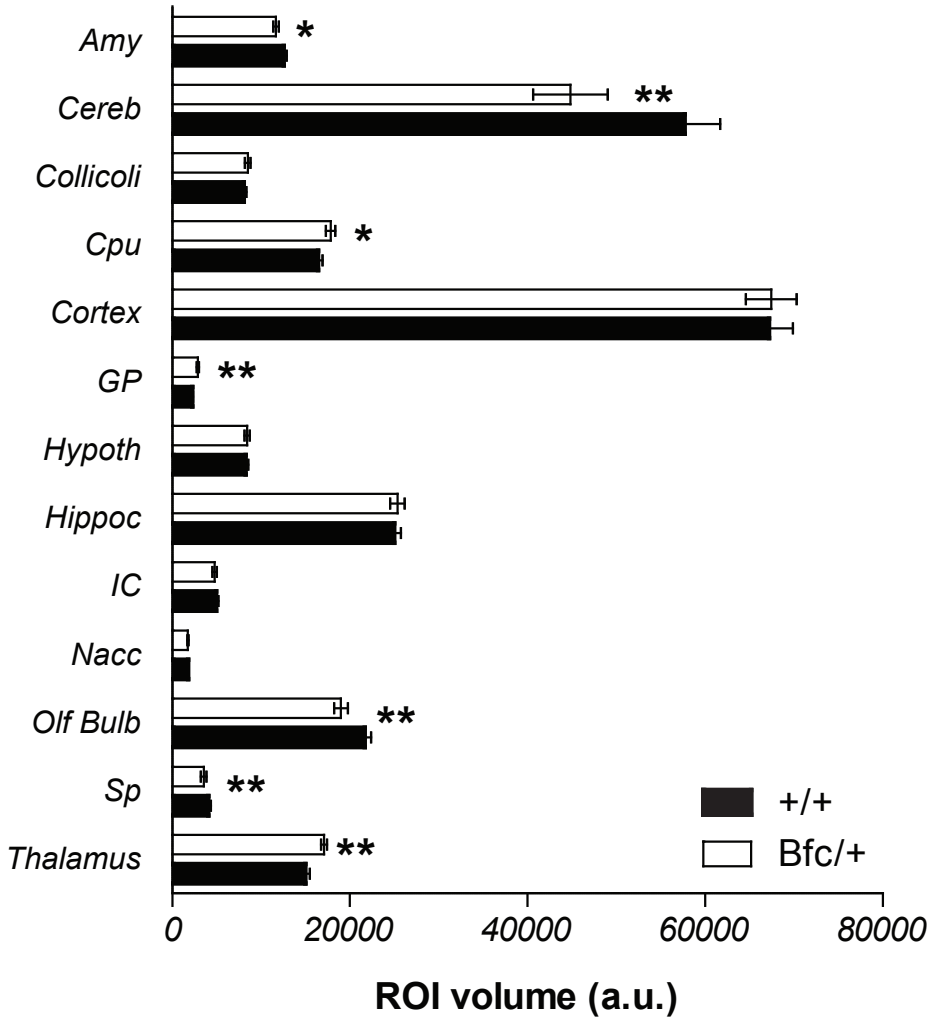

Figure S6. Distinct regional differences in volume measurements detected using MRI. Mean volume of representative brain anatomical structures (regions-of-interest, ROI) in *Bfc/+* mice and control littermates as measured by MRI (mean ± sem). *p<0.05, ** p<0.01 vs. control; one-way ANOVA followed by Fisher's LSD test. Amy: amygdala, Cereb: cerebellum; Cpu: caudate and putamen; GP: globus pallidus; Hippoc: hippocampus; Hipot: hypothalamus; IC: internal capsule; Nacc: nucleus accumbens; Olf Bulb: olfactory bulbs; Sp: septum

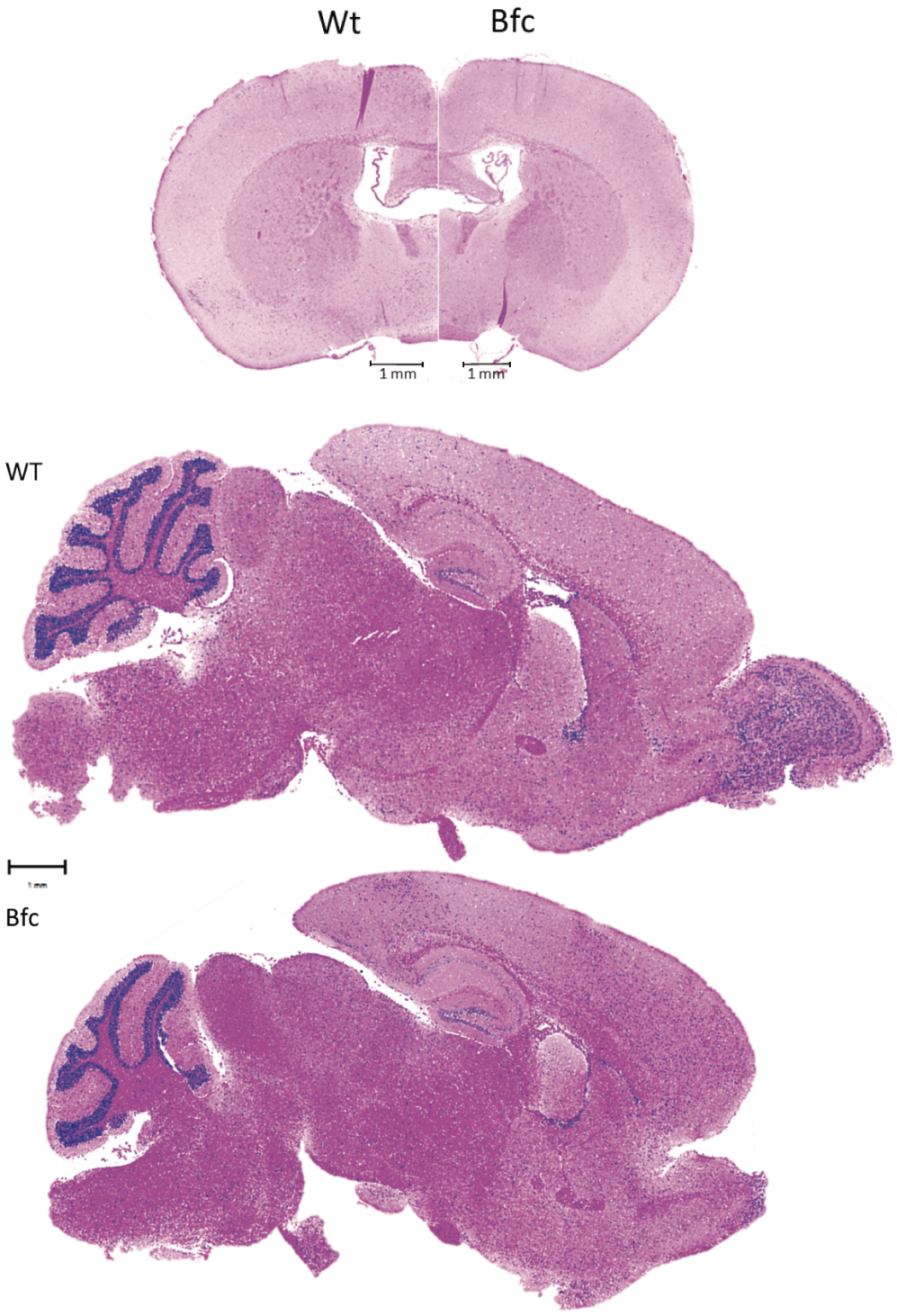

Figure S7. Histological sections of *+/+* and *Bfc/+* brains. Representative coronal and sagital H&E stained sections of *+/+* and *Bfc/+* brains. Note the gross differences in, for example, cerebellum and olfactory bulbs.

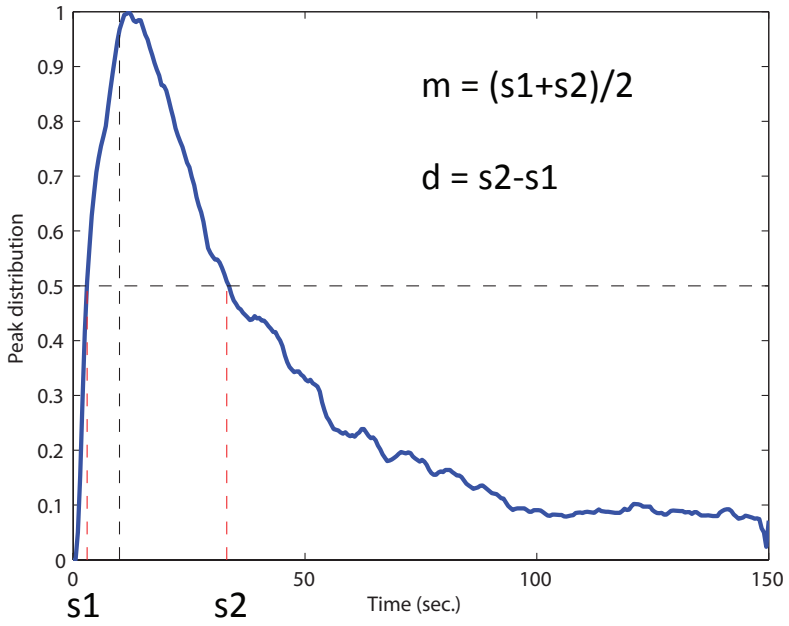

Figure S8. Representative peak distribution of nose pokes. From the distribution of nose pokes during the trials we extracted the start time (s1), the stop time (s2), the peak time (m) and the spread (d).

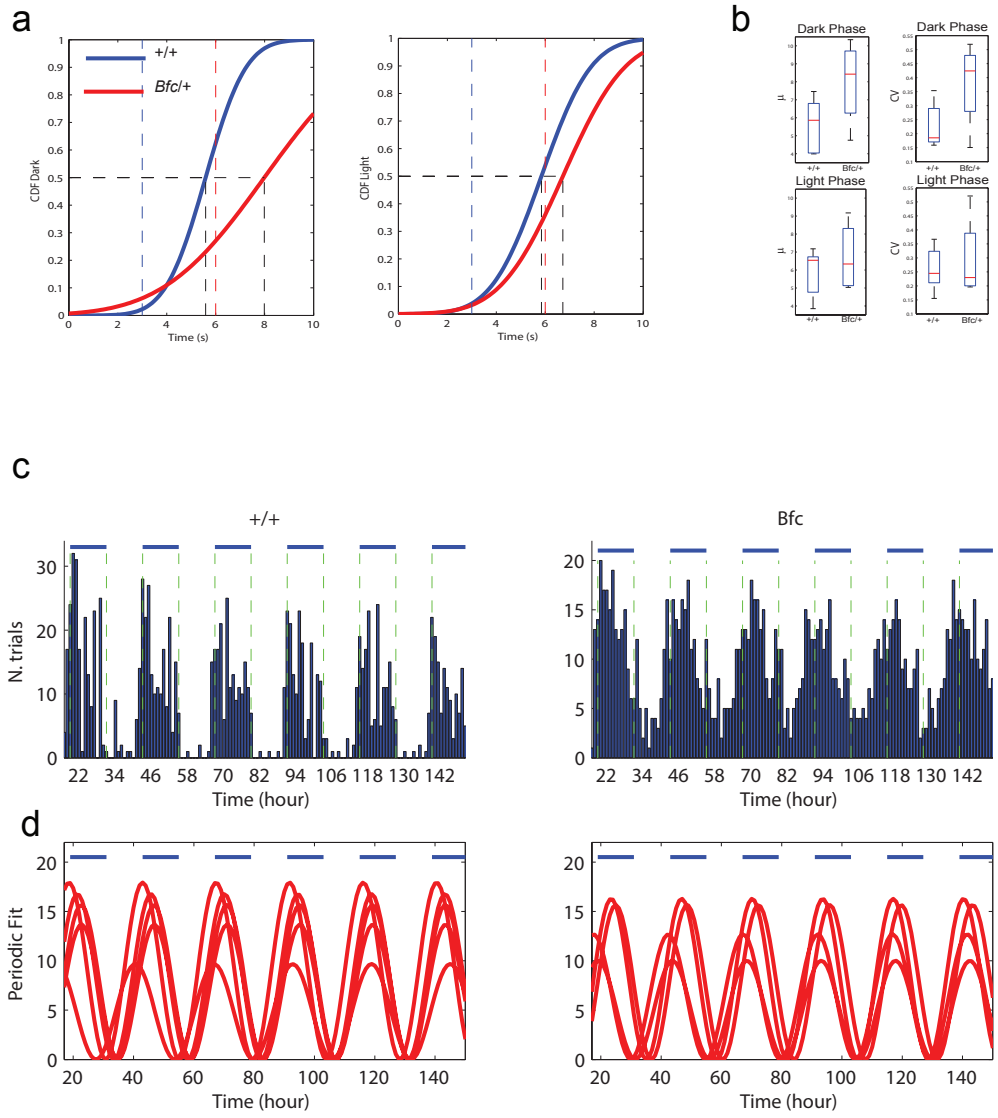

Figure S9. Switch task. (**A**) The cumulative probabilities of switch latencies (the time at which the mouse stops nose poking in the short-location and moves to the long location) as defined in (2). The curves are defined for all dark (left panel) and light (right panel) data and divided between wild-type and *Bfc* mutants. (**B**) From the described cumulative distribution of the switch latencies we have derived the Time Accuracy (TA), as the median ($Q_{0.5}$), and the Time Precision (TP), as the difference of the third and first inter-quartiles ($Q_{0.75}$- $Q_{0.25}$), as described in (3). Box-plots of TAs (the median values for each subject) and TPs (the inter-quartiles) are shown for the dark and light phases. (**C**) Total trials over several days of home-cage testing are represented with two representative subjects (+/+ and Bfc/+). The blue line represents the dark period in which the animals are mostly awake. (**D**) The periodicity of the behavioural performance was computed fitting the activity distributions (shown in **C**) with a periodic function. No circadian differences occur between wild-type and mutant mice.

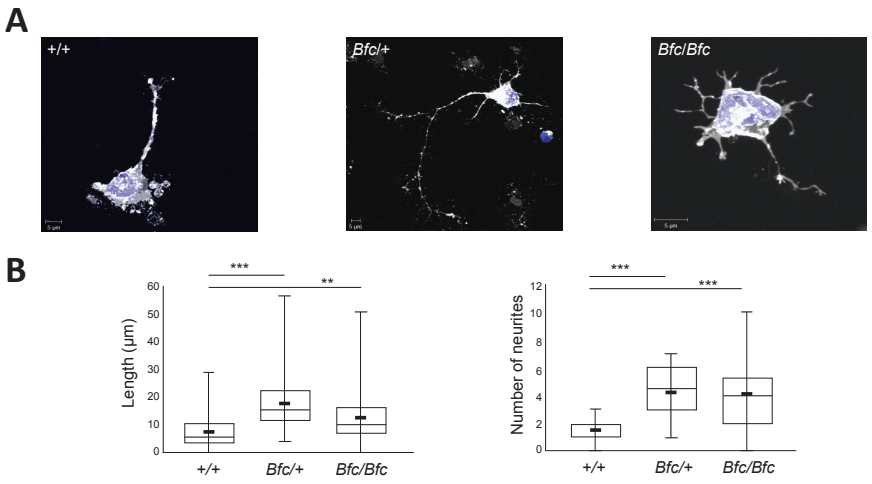

Figure S10. **Morphological and functional deficits in *Bfc/+* primary hippocampal neuronal cultures**. **(A)** Representative images showing neurite arborisation in primary cultures of +/+, *Bfc*/+ and *Bfc*/*Bfc* hippocampal neurons after one day in culture. **(B)** The average length (left panel) and number (right panel) of neurites is significantly greater in *Bfc/+* and *Bfc/Bfc* cultures (**p=0.011, ***p<0.0001).

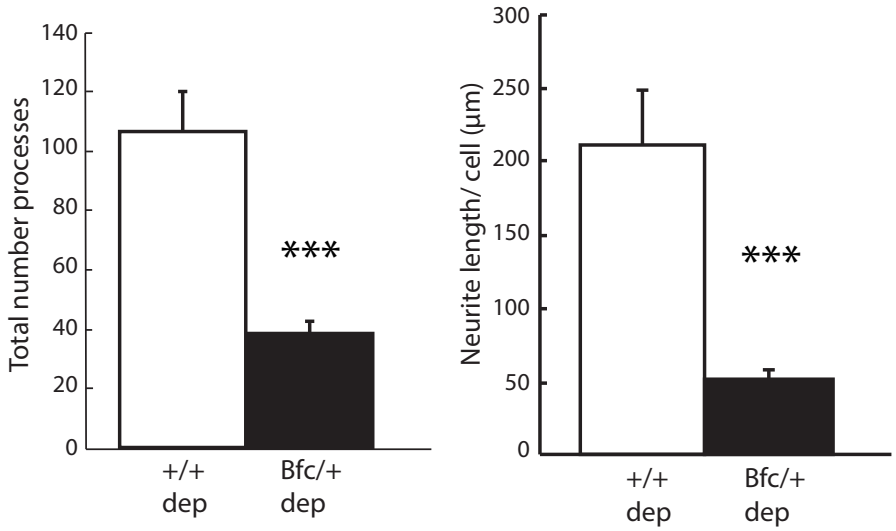

Supplementary Figure 11. **Morphological and functional changes after depolarizing solution application in *Bfc/+* primary hippocampal neuronal cultures**. Number of processes and neurite length per neuron under depolarising (dep) conditions are presented. Processes and total length are significantly reduced in *Bfc/+* neurons. Student T-test, ***p<0.001.

Supplementary Table 1

	experiment	selected active channels	total number of recorded single	number of electrodes recording		
				single units	two units	>two units
+/+	235	141	113	80,0%	18,0%	2,0%
	228	118	104	90,0%	9,0%	1,0%
Bfc/+	242	54	44	81,0%	17,0%	2,0%
	245	258	216	84,0%	14,0%	2,0%
	average	**143**	**119**	**84,0%**	**14,5%**	**1,5%**

Table legend: Spike sorting performances of extracellular signals recorded with high-density electrode arrays from cultured Bfc/+ heterozygous neuronal networks and *+/+* networks, seeded at low cellular density (c.f. Methods section). Spike sorting was performed using the Offline Spike Sorter from Plexon (T-distribution E-M sorting algorithm).

References

1. Xing, Y., Takemaru, K., Liu, J., Berndt, J.D., Zheng, J.J., Moon, R.T., and Xu, W. 2008. Crystal structure of a full-length beta-catenin. *Structure* 16:478-487.
2. Balci, F., Freestone, D., and Gallistel, C.R. 2009. Risk assessment in man and mouse. *Proc Natl Acad Sci U S A* 106:2459-2463.
3. Lassi, G., Ball, S.T., Maggi, S., Colonna, G., Nieus, T., Cero, C., Bartolomucci, A., Peters, J., and Tucci, V. 2012. Loss of Gnas imprinting differentially affects REM/NREM sleep and cognition in mice. *PLoS Genet* 8:e1002706.